Please cite this paper as:
Hawileh R.A., Abdalla J.A., Naser M.Z. (2018). “Modeling the Shear Strength of Concrete Beams Reinforced with CFRP Bars under Unsymmetrical Loading.” Mechanics of Advanced Materials and Structures. pp. 1-8. (https://doi.org/10.1080/15376494.2018.1432803).

Modeling the Shear Strength of Concrete Beams Reinforced with CFRP Bars under Unsymmetrical Loading

R.A. Hawileh[a*], J.A. Abdalla[a], M. Z. Naser[b]

[a] *Department of Civil Engineering, American University of Sharjah, Sharjah P.O.Box 26666, UAE, Tel.: +971 6 515 2496, fax: +971 6 515 2979*

[b]*Post-doctoral Research Fellow, Department of Civil and Environmental Engineering, Michigan State University, US*

* Professor, Corresponding Author, E-mail address: *rhaweeleh@aus.edu*

Abstract

This study presents the development of a nonlinear finite element (FE) model that is capable of simulating the response and predicting the shear strength of concrete beams reinforced with carbon fiber-reinforced polymer (CFRP) bars. More specifically, this paper investigates the effect of unsymmetrical loading which creates two shear span-to-depth (a/d) ratios within the beam specimen and further complicates shear response, especially in FRP-reinforced concrete beams. It is observed that, the predicted FE results are in very close agreement with the measured experimental results. Thus, it can be concluded that the developed models can be used to simulate the behavior of concrete beams reinforced with CFRP bars.

Keywords: Computational modeling; CFRP bars; shear strength; reinforced concrete beams; bond-slip.

This is a preprint draft. The published article can be found at: https://doi.org/10.1080/15376494.2018.1432803

Please cite this paper as:
Hawileh R.A., Abdalla J.A., Naser M.Z. (2018). “Modeling the Shear Strength of Concrete Beams Reinforced with CFRP Bars under Unsymmetrical Loading.” Mechanics of Advanced Materials and Structures. pp. 1-8. (https://doi.org/10.1080/15376494.2018.1432803).

1. Introduction

For the last two decades, researchers and engineers implemented the use of fiber-reinforced polymer (FRP) bars to replace steel bars in reinforcing concrete structural members [1-4]. The two main types of FRP bars commonly used as internal reinforcement are made of Glass (GFRP) or Carbon (CFRP) material. While, GFRP is relatively cheaper than CFRP, GFRP bars have significantly lower elastic modulus which tend to reduce rigidity of the reinforced beam and consequently its ability to retain cracks development. Further, GFRP rebars are prone to long-term material degradation which raises concerns regarding the durability and sustainability of the reinforced beam. In fact, recent tests have shown that unlike glass fibers, carbon fibers cannot absorb moisture and thus are resistant to acid, alkali and organic solvents [5-7]. Hence, CFRP rebars do not undergo sizeable deterioration in saline (marine) environments where humidity is high and or cold regions where salt (and Chloride by-products) are used for deicing. Thus, CFRP bars are recognized as the most favorable material to replace the conventional flexural steel bars in reinforced concrete (RC) slabs and beams due to their high strength-to-weight ratio, resistance to corrosion and durable bond characteristics [5-8]. In addition, the flexural longitudinal CFRP bars in RC members contribute to the concrete shear strength in a similar fashion to that of the steel reinforcement as presented by many researchers [9-12].

The concrete contribution to the shear resistance of RC beams is influenced by the concrete compressive strength, aggregate interlock, dowel action, shear span-to-depth ratio (*a/d*), and beam size. Researchers have examined experimentally and numerically

This is a preprint draft. The published article can be found at: https://doi.org/10.1080/15376494.2018.1432803

Please cite this paper as:
Hawileh R.A., Abdalla J.A., Naser M.Z. (2018). “Modeling the Shear Strength of Concrete Beams Reinforced with CFRP Bars under Unsymmetrical Loading.” Mechanics of Advanced Materials and Structures. pp. 1-8. (https://doi.org/10.1080/15376494.2018.1432803).

the influence of such parameters on the performance of concrete beams reinforced with FRP bars when loaded symmetrically under one-point or two-point loading [13-23]. However, there are limited studies on the shear resistance of such beams when loaded unsymmetrically till failure.

Among the limited studies, Razaqpur et al. [23] studied experimentally the effect of the *a/d* ratio and beam size on the shear resistance of CFRP-reinforced concrete beams subjected to unsymmetrical loading. The beam specimens were designed to fail in shear and subjected to a concentrated load that created two different *a/d* ratios within the same beam specimen till failure. A total of six specimens with four different sizes were cast without shear reinforcement and tested under one concentrated load and with three different *a/d* ratios. The depth of four RC beam specimens was varied from 200 mm to 500 mm. The test results indicated that the *a/d* ratio and beam size have a major effect on the shear strength of RC beams. It is also noteworthy that the ACI-440 [24] guidelines for calculating the concrete shear strength overestimated the obtained experimental values for the large size beams. Thus, the current ACI-440 design guidelines for calculating the concrete shear strength should be modified to include these two parameters (*a/d* ratio and beam size) as suggested by the authors [23].

Three-dimensional nonlinear finite element (FE) modeling and analysis of concrete beams reinforced with CFRP bars will contribute to the understanding of the behavior of such beams under unsymmetrical loading. Full range of data representing deformation and stress results will be obtained from the developed FE models. This is advantageous over the expensive and time consuming experimental testing that is limited to deflection and strain results of LVDTs and strain gauges at discrete and limited locations within the tested specimens.

The main objective of this work is to determine the effects of shear span-to-depth ratio and beam depth on the concrete contribution to the shear resistance of concrete beams longitudinally reinforced with CFRP bars. This study highlights the fact that the failure load and location in analyzed beams cannot be properly predicted by the shear design recommendations of American Concrete Institute (ACI) Committee 440 as these provisions do not account for the effects of span-to-depth ratio and beam size on shear strength of FRP-reinforced concrete beams. Thus, this study aims at developing six FE models using the finite element software, ANSYS version 14.5 [21] that can predict the response and concrete shear strength of concrete beams reinforced with CFRP bars and subjected to unsymmetrical loading. In order to validate the accuracy of the developed models, the predicted load versus maximum deflection results, load-carrying capacity, shear force at the left support (V_L), shear force at the right support (V_R), and ultimate shear strength (V_u) are compared with the obtained experimental results of Razaqpur et al. [23]. The developed FE models incorporated the nonlinear properties of the concrete material in both tension and compression and the elastic-brittle material properties of the CFRP

Please cite this paper as:
Hawileh R.A., Abdalla J.A., Naser M.Z. (2018). "Modeling the Shear Strength of Concrete Beams Reinforced with CFRP Bars under Unsymmetrical Loading." Mechanics of Advanced Materials and Structures. pp. 1-8. (https://doi.org/10.1080/15376494.2018.1432803).

bars. The bond-slip behavior between the CFRP bars and concrete surfaces is also incorporated in the developed models.

2. Summary of Experimental Program

A total of six concrete beams reinforced with CFRP bars that were cast and tested under unsymmetrical one-point loading by Razaqpur et al. [23] were simulated in this study. The variables of the test program were the *a/d* ratio and beam size or depth. All beams were reinforced with the same amount of CFRP reinforcement ratio (about 0.3%) and concrete strength (average strength of 52.3 MPa) to study the effect of *a/d* ratio and beam size on the concrete shear strength of the tested specimens. The CFRP bars had a diameter and cross-sectional area of 9.5 mm and 72 mm^2, respectively. The width, span length, and total length of the six beam specimens were 300 mm, 3,000 mm, and 3,630 mm, respectively.

The beams' designation, height h, depth d, area of CFRP bars A_f, shear span to the left support a_L, and shear span to the right support a_R are provided in Table 1. The tested beam specimens were designed and cast without internal stirrups to fail in shear. It is clearly indicated in Table 1 that the beams were divided into two groups to examine the influence of the beam size and *a/d* ratio on the shear strength of the tested specimens. More details of the experimental program and test matrix can be found in the work conducted by Razaqpur et al. [23].

Table 1: Detailing of tested beam specimens [23]

Beam	h (mm)	d (mm)	A_f (mm^2)	a_L (mm)	a_L/d	a_R (mm)	a_R/d
B1	230	200	210	700	3.5	2,300	11.5
B2	330	300	288	1,050	3.5	1,950	6.5
B3	430	400	360	1,400	3.5	1,600	4.0
B4	530	500	420	1,750	3.5	1,250	2.5
B5	430	400	360	2,600	6.5	400	1.0
B6	430	400	360	2,400	6.0	600	1.5

3. Development of Finite Element Models

3.1. Element Types

A total of six FE 3D models are developed to predict the shear strength of the tested specimens described in the previous section. The models are created and analyzed in the ANSYS 14.5 [25] software. The assigned geometry, material properties, loading, and boundary conditions to the developed FE models resembled that of the tested specimens. The developed models are designated as “B1_FE”, “B2_FE”, “B3_FE”, “B4_FE”, “B5_FE”, and “B6_FE”, respectively.

Figure 1 shows the isometric view and cross-sections of the optimum mesh for every RC beam specimens, respectively. The obtained optimum mesh of every beam shown in Fig. 1 has been obtained by conducting a mesh sensitivity analysis. The concrete brick element, SOLID65 [25] is used to model the concrete beam. The element is defined using eight nodes, each with 3 degrees of freedom (*dof*) along the x, y, and z directions, respectively. This element is also capable of simulating the nonlinear properties of concrete in tension and compression [25]. The longitudinal CFRP bars are simulated using LINK180 [25] elements that is capable of simulating the elastic-brittle properties of the FRP reinforcement. The loading plates and supports are modelled using brick SOLID45 [25] elements. The properties of this element are similar to that of the SOLID65 but without the capability of simulating the nonlinear behavior of concrete. This technique will eliminate stress concentration problems at the concrete surfaces under the loading plates. SOLID45 [25] elements are utilized to model the loading supports shown in Fig. 1. The properties of SOLID45 element is similar to SOLID65, but without the cracking and crushing capabilities.

The bond-slip behavior between the CFRP bars and adjacent concrete surfaces is also incorporated in the developed FE models. The CEB-FIP [26] bond-slip model presented in Eqs. (1-4) is used to develop the complete bond-slip behavior between the CFRP bars and concrete interface.

$$\tau = \tau_{\max}\left(\frac{s}{s_1}\right)^{0.4} \qquad for \quad 0 \le s \le s_1 \qquad (1)$$

$$\tau = \tau_{\max} \qquad for \quad 0 \le s \le s_1 \qquad (2)$$

$$\tau = \tau_{\max}(\tau_{\max} - \tau_f)\frac{(s - s_2)}{(s_3 - s_2)} \qquad for \quad 0 \le s \le s_1 \qquad (3)$$

$$\tau = \tau_f \qquad for \quad 0 \le s \le s_1 \qquad (4)$$

where,

τ = bond stress in (MPa)

s_1, s_2, s_3 = relative slip in (mm)

$\tau_{max} = 2.5\sqrt{f_c'}$ = maximum bond stress in (MPa)

s_{max} = slip in (mm) corresponding to τ_{max}

$\tau_f = 0.4\tau_{max}$ = bond stress at failure in (MPa)

The used values of τ_{max} and s_{max} for the CFRP bars were taken from as results of number of experimental tests [27-32] as 15.24 MPa and 2.8 mm, respectively. The spring element COMBIN14 [25] is used to simulate the bond-slip behavior along the longitudinal axis of the CFRP bars. In addition, the *dof* of the adjacent nodes of the SOLID65 and LINK180 elements were assumed to be fully compatible along the other two translational directions (*y and z*). This is achieved by coupling the adjacent nodes along these directions.

3.2. Material Properties and Constitutive laws

The incorporated material properties in the developed FE models are similar to that of the tested beam specimens and consider the nonlinear material of concrete in compression, concrete cracking, and brittle failure of the CFRP bars in tension.

Figure 2 shows the employed stress-strain curves of concrete in compression and tension. The nonlinear material properties in compression and tension are based on the Hognestad [33] parabola and William and Warnke [34] model, respectively. The elastic modulus, Poisson’s ratio, tensile strength, and compressive strength of the tested beam were taken as 33.99 GPa, 0.2, 4.34 MPa, and 52.3 MPa, respectively. The concrete constitutive model in ANSYS also requires inputs of coefficients for the open and close cracks, β_t and β_c, that range between 0.0 and 1.0. The 0.0 and 1.0 values represent smooth

Please cite this paper as:
Hawileh R.A., Abdalla J.A., Naser M.Z. (2018). “Modeling the Shear Strength of Concrete Beams Reinforced with CFRP Bars under Unsymmetrical Loading.” Mechanics of Advanced Materials and Structures. pp. 1-8. (https://doi.org/10.1080/15376494.2018.1432803).

(full loss of shear transfer) and rough (no loss of shear transfer) cracks, respectively. Based on an extensive parametric study by the authors [35-37] on simulating the response of shear-deficient RC beams, the β_t and β_c coefficients were taken as 0.2 in this study.

In addition, elastic-brittle material properties were assigned to the CFRP longitudinal rebar reinforcement, with an elastic modulus, Poisson’s ratio, and tensile strength of 114 GPa, 1500 MPa, and 0.28, respectively. Moreover, the assigned elastic modulus and Poisson’s ratio of the rigid loading supports were taken as 200 GPa and 0.3, respectively.

3.3. Convergence and failure criteria

The developed FE models were analyzed by applying the load incrementally till failure using the load steps and substeps commands in ANSYS [25]. The program uses the applied cyclic loads were divided into a series of load increments called load steps and substeps. At the end of each load increment, convergence is achieved by Newton-Raphson equilibrium iterations. The minimum load substep was taken as 10 N and divergence occurred when the solution for the 10 N load increment does not satisfy the equilibrium equations and falls outside the radius of convergence. In general, failure in the developed models is said to occur once the shear capacity of the analyzed falls below the level of applied loading [35-37]. At this point, stiffness of the elements located in high shear region drastically drops to zero. This hinders stability of the numerical solution and leads to failure (divergence due to loss of shear capacity).

This is a preprint draft. The published article can be found at: https://doi.org/10.1080/15376494.2018.1432803

Please cite this paper as:
Hawileh R.A., Abdalla J.A., Naser M.Z. (2018). “Modeling the Shear Strength of Concrete Beams Reinforced with CFRP Bars under Unsymmetrical Loading.” Mechanics of Advanced Materials and Structures. pp. 1-8. (https://doi.org/10.1080/15376494.2018.1432803).

4. Results and discussion

4.1. Model validation

In order to validate the accuracy of the developed FE models, the experimental and numerically predicted applied load versus maximum deflection response curves are compared, as shown in Fig. 3. The horizontal location of the measured deflection point away from the left support (at a distance x) for each beam specimen is also indicated in Fig. 3. In addition, the measured and predicted results for the load-carrying capacity (P), shear force at left support (V_L) at failure, and shear force at right support (V_R) at failure are compared and presented in Table 2.

It can be observed from Fig. 3 that there is a reasonable agreement between the measured and predicted load versus maximum deflection response curves for all the tested specimens. In addition, it is clearly indicated from Table 2 that the maximum Mean Absolute Percent Error (MAPE) between the predicted and measured results is less than 13.5% for P, V_L, and V_R. In particular, as indicated in Table 2, the average MAPE between the predicted and measured P, V_L, and V_R values are 6.29%, 6.34% and 6.82%, respectively. The Normalized Mean Square Error (NMSE) between the predicted and measured P, V_L, and V_R are 0.02, 0.66 and 0.01, respectively while the correlation coefficients (R) of P, V_L, and V_R are 0.998, 0.758 and 0.999, respectively.

Thus, it could be concluded that the developed models are very accurate and can confidently be used to predict the shear strength and performance of concrete beams reinforced with CFRP bars and subjected to unsymmetrical loading.

4.2. Model Behavior

The developed FE models can provide full field of deformation and stress results. This is advantageous over experimental testing that is limited to deformation and strain results at discrete locations within the beam specimen. For instance, Figure 4 shows the distribution of the principle tensile stress (σ_3) throughout the tested beam specimens. The six tested beam specimens failed by a major diagonal crack between the support and loading point. The distributions of the principle tensile stresses in Fig. 4 of the developed models clearly indicate such failure mechanism.

Figure 5 shows the axial stress distribution in the CFRP bars at failure. It can be observed from Fig. 5 that the stress in the bars is less than the tensile strength of the CFRP bars (1500 MPa). Thus, it could be concluded that none of the CFRP bars failed during testing.

5. Conclusion

This numerical study presented the development of six 3D FE models to simulate the response of concrete beams reinforced with CFRP bars when subjected to unsymmetrical loading. The following observations and conclusions were drawn:

Please cite this paper as:
Hawileh R.A., Abdalla J.A., Naser M.Z. (2018). "Modeling the Shear Strength of Concrete Beams Reinforced with CFRP Bars under Unsymmetrical Loading." Mechanics of Advanced Materials and Structures. pp. 1-8. (https://doi.org/10.1080/15376494.2018.1432803).

- The models can predict the load versus maximum deflection response curves of the tested specimens with a reasonable level of accuracy.

- The developed FE models are capable of predicting the load-carrying capacity, shear strength at left support, and shear strength at right support of the tested specimens with good accuracy.

- The MAPE between the predicted and measured values ranged from 13.19% to 0.25% for the load-carrying capacity, from 13.11% to 0.97% for shear strength at the left support and from 13.33% to 0.74% for shear strength at the right support.

- The NMSE of the predicted P, V_L, and V_R are 0.02, 0.66 and 0.01, respectively, indicating that P and V_R were predicted very accurately.

- The correlation between the predicted and measured values, especially for P and V_R are almost = 1.0.

- It should be noted that shear strength in beams similar to those presented in this study is a function of numerous factors such as aggregate size, concrete compressive strength, ratio of the longitudinal reinforcement etc. Hence, the authors urge the civil engineering community to study the effects of such parameters in order to better understand the shear strength behavior of concrete beams reinforced with FRP rebars.

Please cite this paper as:
Hawileh R.A., Abdalla J.A., Naser M.Z. (2018). "Modeling the Shear Strength of Concrete Beams Reinforced with CFRP Bars under Unsymmetrical Loading." Mechanics of Advanced Materials and Structures. pp. 1-8. (https://doi.org/10.1080/15376494.2018.1432803).

References

[1] H. Akbarzadeh, A.A. Maghsoudi, "Experimental and analytical investigation of reinforced high strength concrete continuous beams strengthened with fiber reinforced polymer", Materials & Design, 31(3), 1130-1147, 2010.

[2] R.A. Hawileh, "Finite element modeling of reinforced concrete beams with a hybrid combination of steel and aramid reinforcement", Materials & Design, 65, 831-839, 2015.

[3] Czesław Bywalski, Michał Drzazga, Mieczysław Kamiński, Maciej Kaźmierowski, "Analysis of calculation methods for bending concrete elements reinforced with FRP bars", Archives of Civil and Mechanical Engineering, 16(4), 901-912, 2016.

[4] A.K. EL-Sayed, B. Benmokrane, "Evaluation of the new Canadian highway bridge design shear provisions for concrete beams with fiber-reinforced polymer reinforcement", Canadian Journal of Civil Engineering, 35(6), 609-623, 2008.

[5] T.H. Almusallam, Y.A. Al-Salloum, "Durability of GFRP rebars in concrete beams under sustained loads at severe environments", J Compos Mater, 40(7), 623-637, 2006.

[6] M.L. Porter, B.A. Barnes, "Accelerated Aging Degradation of Glass Fiber Composites, In: Second International Conference on Composites in Infrastructure", ICCI'98, Tucson, AZ, , 446–459, 1998.

[7] F. Ellyin, C. Rohrbacher, "Effect of aqueous environment and temperature on glass-fibre epoxy resin composites". J. Reinf. Plast. Compos., 19(17), 1405–1427, 2000.

[8] A. Lapko, M. Urbański, "Experimental and theoretical analysis of deflections of concrete beams reinforced with basalt rebar", Archives of Civil and Mechanical Engineering, 15(1), 223-230, 2015.

[9] Z. Omeman, M. Nehdi, H. EL Chabi, "Experimental study on the shear behaviour of CFRP-reinforced concrete short beams", Canadian Journal of Civil Engineering, 35(1), 1-10, 2008.

[10] R. Hawileh, M. Naser, "Thermal-Stress Analysis of RC Beams Reinforced with GFRP Bars", Composites Part B: Engineering, 43(5), 2135-2142, 2012. https://doi.org/10.1016/j.compositesb.2012.03.004

[11] M.Z. Naser, R.A. Hawileh, J.A. Abdalla, A. Al-Tamimi, "Bond Behavior of CFRP Cured Laminates: Experimental and Numerical Investigation", Journal of Engineering Materials and Technology, ASME, 134, 2012. https://doi.org/10.1115/1.4003565

[12] T. Trapko, M. Musial, "The effectiveness of CFRP materials strengthening of eccentrically compressed reinforced concrete columns", Archives of Civil and Mechanical Engineering, 11(1), 249-262, 2011.

[13] A.G. Razaqpur, O.B. Isgor, "Proposed shear design method for FRP-reinforced concrete members without stirrups", ACI Structural Journal, 103(1), 93-102, 2006.

[14] T. Shioya, "Shear properties of large reinforced concrete members", Special Report No. 25, Institute of Technology, Shimizu Corporation, Tokyo, 1989.

[15] A. Tureyen, R.J. Frosch, “Shear tests of FRP-reinforced beams without stirrups”, ACI Structural Journal, 99(4), 427-434, 2002.

[16] A.K. El-Sayed, E. El-Salakawy, B. Benmokrane, “Shear capacity of high-strength concrete beams reinforced with FRP bars”, ACI Structural Journal, 103(3), 383–389, 2006.

[17] A.G. Razaqpur, B.B. Isgor, S. Greenaway, A. Selley, “Concrete contribution to the shear resistance of fiber reinforced polymer reinforced concrete members”, Journal of Composites for Construction, 8(5), 452-460, 2004.

[18] G. Mazzucco, V.A. Salomoni, C.E. Majorana, “Three-dimensional contact-damage coupled modelling of FRP reinforcements – simulation of delamination and long-term processes”, Computers and Structures, 110-111, 15-31, 2012.

[19] A. Godat, P. Labossière, K.W. Neale, O. Chaallal, “Behavior of RC members strengthened in shear with EB FRP: Assessment of models and FE simulation approaches”, Computers and Structures, 92-93, 269-286, 2012.

[20] R. Hawileh, J.A. Abdalla, M.H. Tanarslan, M. Naser, “Modeling of Nonlinear Cyclic Response of Shear-Deficient RC T-beams Strengthened with Side Bonded CFRP Fabric Strips”, Computers and Concrete, 8(2), 193-206, 2010. DOI: 10.12989/cac.2011.8.2.193

[21] A. Godat, O. Chaallal, K.W. Neale, “Nonlinear finite element models for the embedded through-section FRP shear-strengthening method”, Computers and Structures, 119, 12-22, 2013.

Please cite this paper as:
Hawileh R.A., Abdalla J.A., Naser M.Z. (2018). "Modeling the Shear Strength of Concrete Beams Reinforced with CFRP Bars under Unsymmetrical Loading." Mechanics of Advanced Materials and Structures. pp. 1-8. (https://doi.org/10.1080/15376494.2018.1432803).

[22] G. Sakar, R. Hawileh, M. Naser, J.A. Abdalla, M. Tanarslan, "Nonlinear Behavior of Shear Deficient RC Beams Strengthened with Near Surface Mounted Glass Fiber Reinforcement under Cyclic Loading" Materials and Design, 61, pp. 16-25, 2014. https://doi.org/10.1016/j.matdes.2014.04.064

[23] A.G. Razaqpur, M. Shedid, B. Isgor, "Shear strength of fiber-reinforced polymer reinforced concrete beams subject to unsymmetric loading" Journal of Composites for Construction, ASCE, 15(4), 500-512, 2011.

[24] American Concrete Institute (ACI) Committee 440, "Guide for the design and construction of concrete reinforced with FRP bars", ACI 440.1R-06, Farmington Hills, MI, 2006.

[25] ANSYS – Release Version 14.5. A Finite Element Computer Software and User Manual for Nonlinear Structural Analysis, ANSYS 2013, Inc. Canonsburg, PA.

[26] Comite Euro-International du Beton (CEB-FIP). CEB-FIP model code 1990. Bulletin D'Information No. 213/214 (Concrete Structures), Lausanne, Switzerland; 1993.

[27] J. Lee, T. Kim, C. Yi, J. Park, Y. You, Y. Park, "Interfacial bond strength of glass fiber reinforced polymer bars in high-strength concrete" Composites Part B: Engineering, 39, 258-270, 2008.

[28] Z. Achillides, K. Pilakoutas, "Bond Behavoiur of Fiber Reinforced Polymer Bars under Direct Pullout Conditions" Journal of Composites for Construction, ASCE, 8(2),173-181, 2004.

[29] A. Belarbi, H. Wang, “Bond-slip response of FRP reinforcing bars in fiber reinforced concrete under direct pullout” In Proceedings of ICFRC-international conference on fiber composites, high performance concretes and smart materials, Chennai, India.

[30] L.J. Malvar, J.V. Cox, K.B. Cochran, K. B. “Bond between carbon fiber reinforced polymer bars and concrete. I: Experimental study”. Journal of composites for construction, 7(2), 154-163, 2003.

[31] M. Baena, L. Torres, A. Turon, C. Barris, “Experimental study of bond behaviour between concrete and FRP bars using a pull-out test”. Composites Part B: Engineering, 40(8), 784-797, 2009.

[32] R. Okelo, R.L. Yuan, “Bond strength of fiber reinforced polymer rebars in normal strength concrete”. Journal of composites for construction, 9(3), 203-213, 2005.

[33] E. Hognestad, N.W. Hanson, D. McHenry, “Concrete stress distribution in ultimate strength design” ACI Journal, 52(12), 455–79, 1955.

[34] K.J. Willam, E.D. Warnke, “Constitutive model for the triaxial behavior of concrete” In: Proceedings international association for bridge and structural engineering. Bergamo (Italy): ISMES; 1975. p. 174.

[35] R. Hawileh, J.A. Abdalla, M.H. Tanarslan, “Modeling of Nonlinear Response of R/C Shear Deficient T-Beam Subjected to Cyclic Loading”, Computers and Concrete, 10(4), 413-428, 2012.

[36] R. Hawileh, J.A. Abdalla, M.Z. Naser, M. Tanarslan, “Finite Element Modeling of Shear Deficient RC Beams Strengthened with NSM CFRP Rods under Cyclic

Please cite this paper as:
Hawileh R.A., Abdalla J.A., Naser M.Z. (2018). "Modeling the Shear Strength of Concrete Beams Reinforced with CFRP Bars under Unsymmetrical Loading." Mechanics of Advanced Materials and Structures. pp. 1-8. (https://doi.org/10.1080/15376494.2018.1432803).

Loading." *ACI Special Publications*: Modeling of FRP Strengthening Techniques in Concrete Infrastructure. 2014.

[37] R. Hawileh, J.A. Abdalla, J., "Finite Element Modeling of the Shear Strength of Concrete Beams Reinforced with CFRP Bars under Unsymmetrical Loading." In: Topping BHV, editor, CCP: 108, Proceedings of the Fourteenth International Conference on Civil, Structural and Environmental Engineering Computing, Stirlingshire (UK): Civil-Comp Proceedings, ISSN 1759-3433; 2015 [paper 193], Edited by: J. Kruis, Y. Tsompanakis and B.H.V. Topping, doi:10.4203/ccp.108.193.

Please cite this paper as:
Hawileh R.A., Abdalla J.A., Naser M.Z. (2018). “Modeling the Shear Strength of Concrete Beams Reinforced with CFRP Bars under Unsymmetrical Loading.” Mechanics of Advanced Materials and Structures. pp. 1-8. (https://doi.org/10.1080/15376494.2018.1432803).

List of Figures:

Please cite this paper as:
Hawileh R.A., Abdalla J.A., Naser M.Z. (2018). "Modeling the Shear Strength of Concrete Beams Reinforced with CFRP Bars under Unsymmetrical Loading." Mechanics of Advanced Materials and Structures. pp. 1-8. (https://doi.org/10.1080/15376494.2018.1432803).

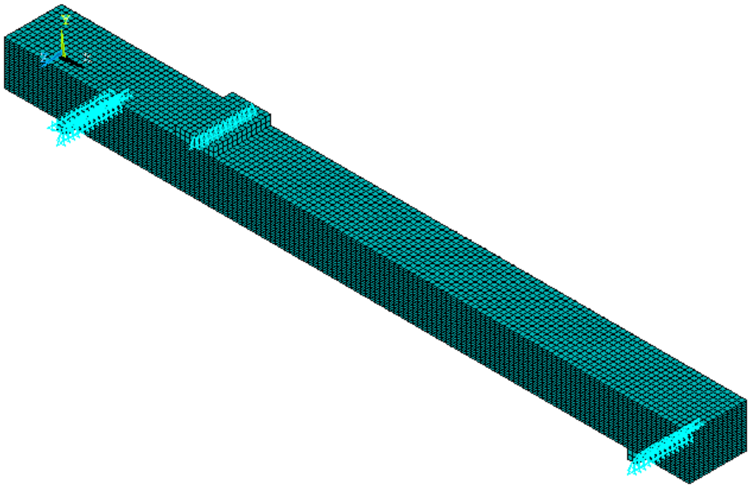

(a) B1_FE

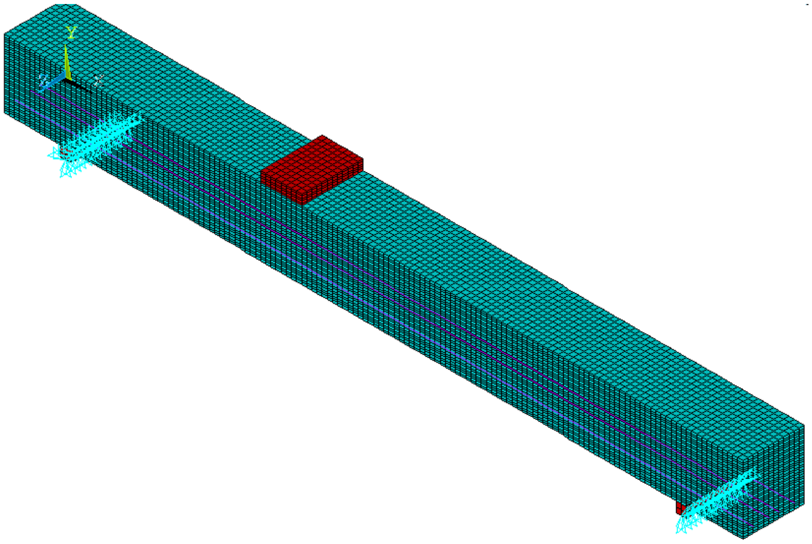

(b) B2_FE

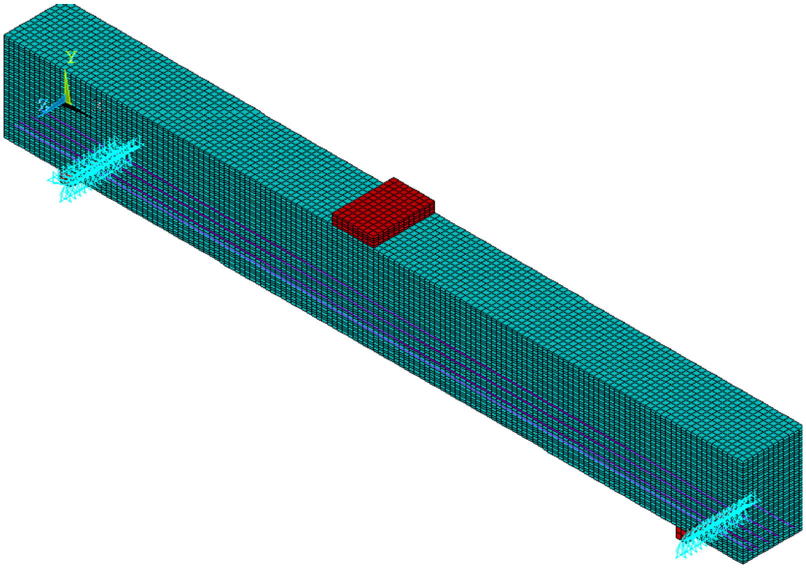

(c) B3_FE

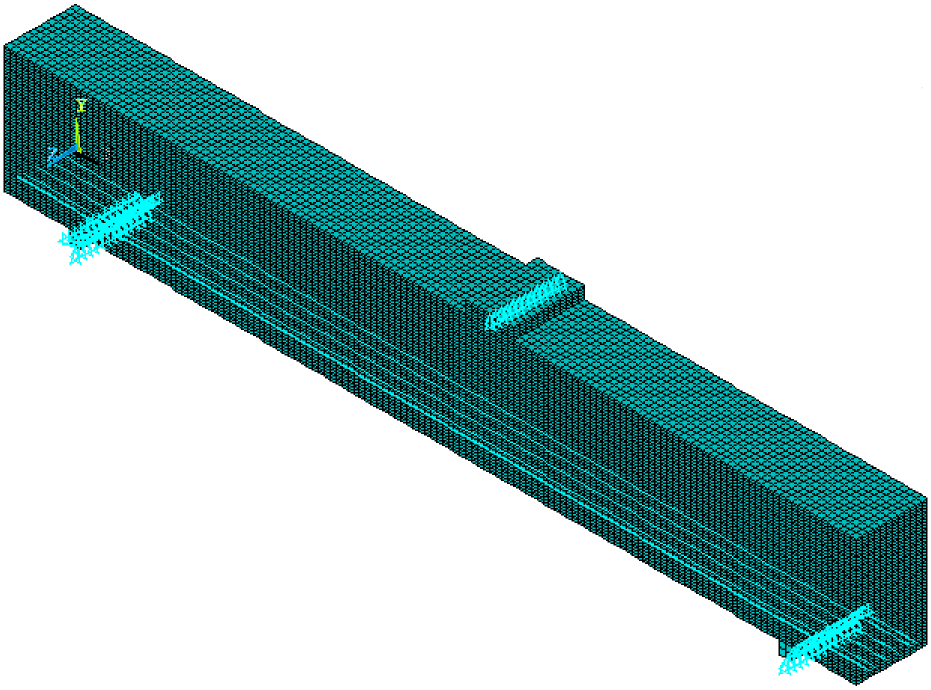

(d) B4_FE

Please cite this paper as:
Hawileh R.A., Abdalla J.A., Naser M.Z. (2018). “Modeling the Shear Strength of Concrete Beams Reinforced with CFRP Bars under Unsymmetrical Loading.” Mechanics of Advanced Materials and Structures. pp. 1-8. (https://doi.org/10.1080/15376494.2018.1432803).

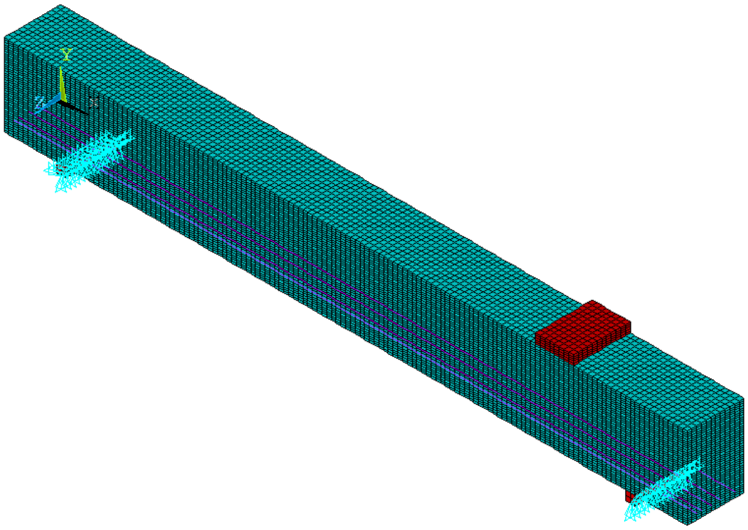

(e) B5_FE

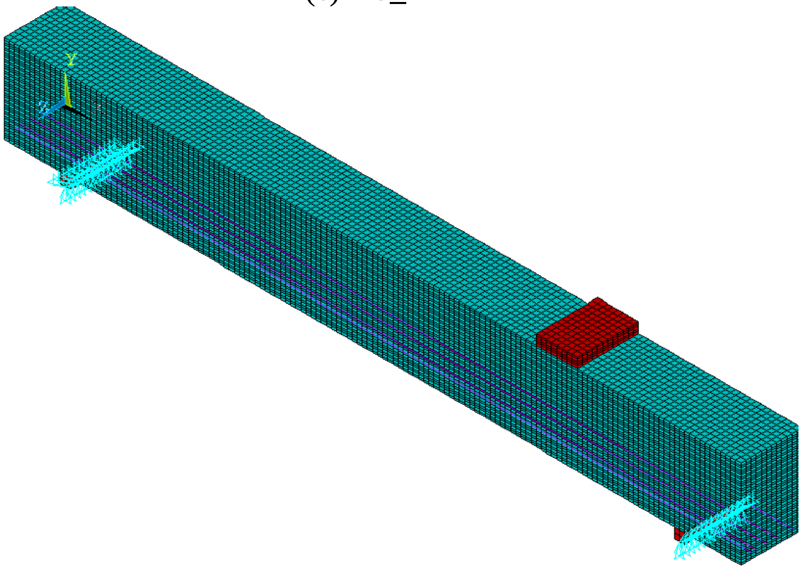

(f) B6_FE

Figure 1: Developed FE models

This is a preprint draft. The published article can be found at: https://doi.org/10.1080/15376494.2018.1432803

Please cite this paper as:
Hawileh R.A., Abdalla J.A., Naser M.Z. (2018). “Modeling the Shear Strength of Concrete Beams Reinforced with CFRP Bars under Unsymmetrical Loading.” Mechanics of Advanced Materials and Structures. pp. 1-8. (https://doi.org/10.1080/15376494.2018.1432803).

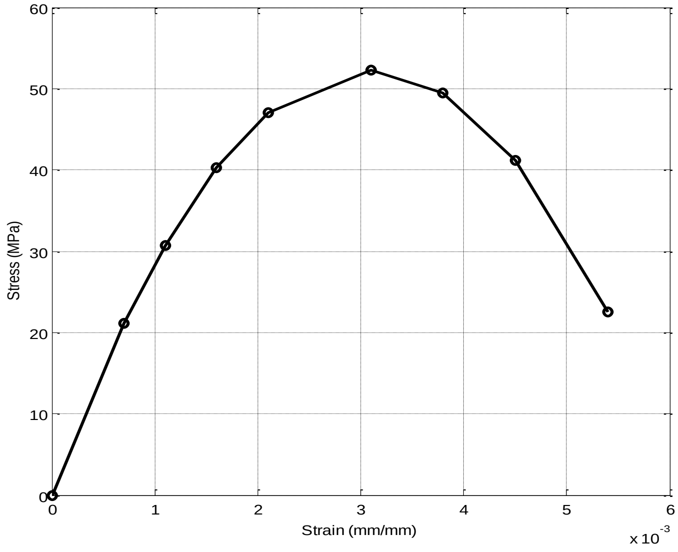

(a) Compressive

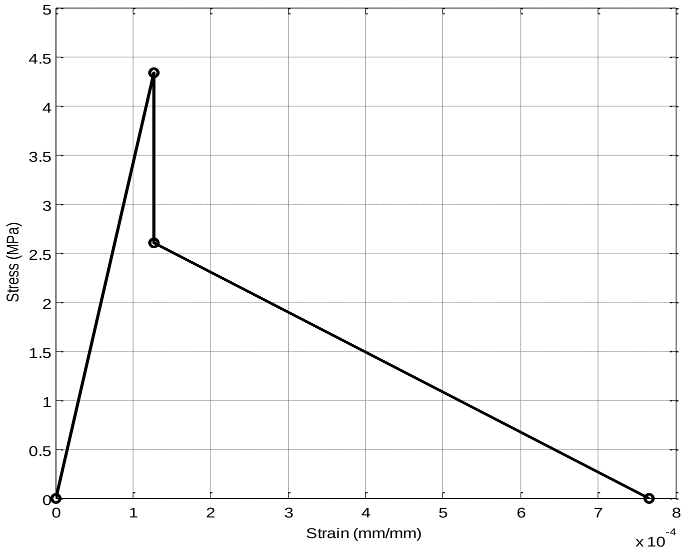

(b) Tensile

Figure 2: Compressive and tensile stress-strain relationships for the concrete

This is a preprint draft. The published article can be found at: https://doi.org/10.1080/15376494.2018.1432803

Please cite this paper as:
Hawileh R.A., Abdalla J.A., Naser M.Z. (2018). "Modeling the Shear Strength of Concrete Beams Reinforced with CFRP Bars under Unsymmetrical Loading." Mechanics of Advanced Materials and Structures. pp. 1-8. (https://doi.org/10.1080/15376494.2018.1432803).

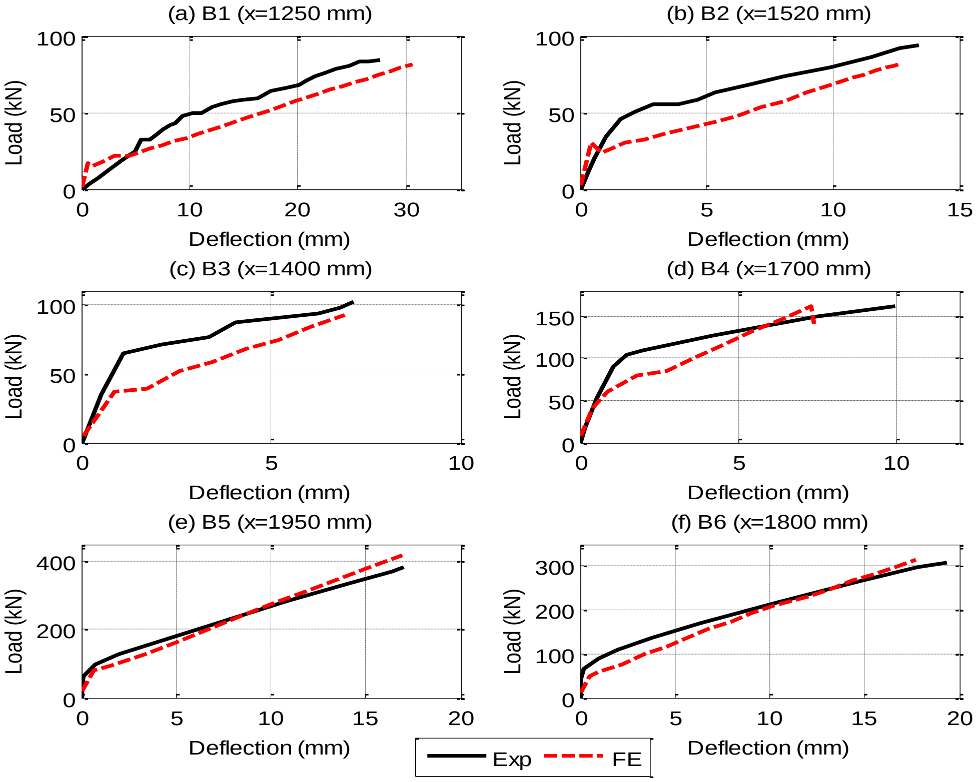

Figure 3: Measured and predicted load versus maximum deflection curves

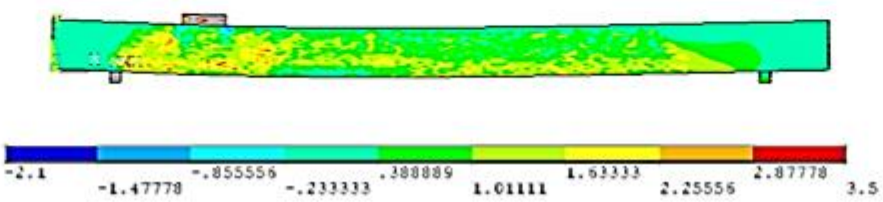
-2.1
-1.47778
-.855556
-.233333
.388889
1.01111
1.63333
2.25556
2.87778
3.5

(B1)

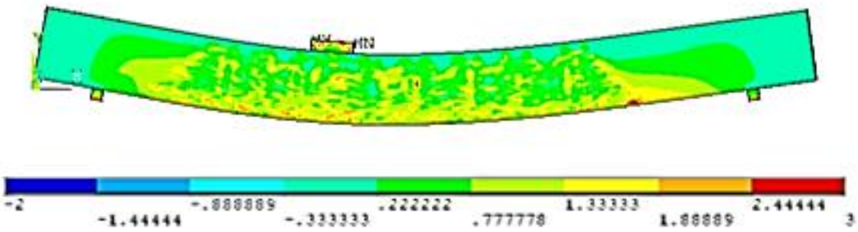
MN
MX
-2
-1.44444
-.888889
-.333333
.222222
.777778
1.33333
1.88889
2.44444
3

(B2)

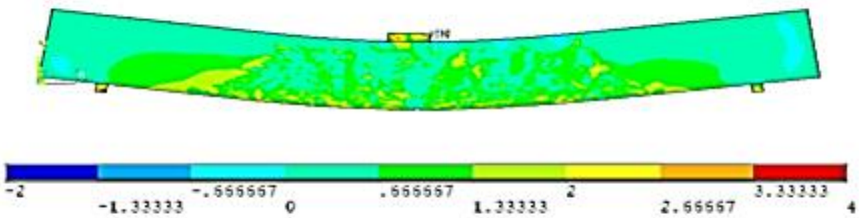
MN
-2
-1.33333
-.666667
0
.666667
1.33333
2
2.66667
3.33333
4

(B3)

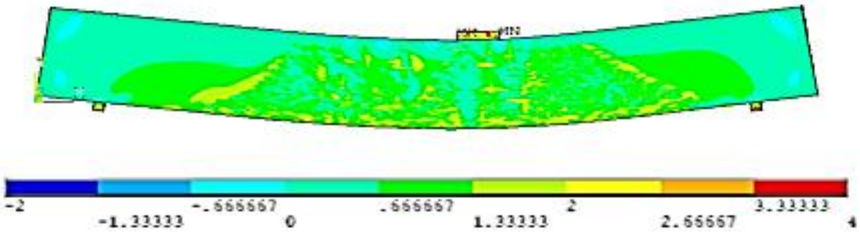
MX
MN
-2
-1.33333
-.666667
0
.666667
1.33333
2
2.66667
3.33333
4

(B4)

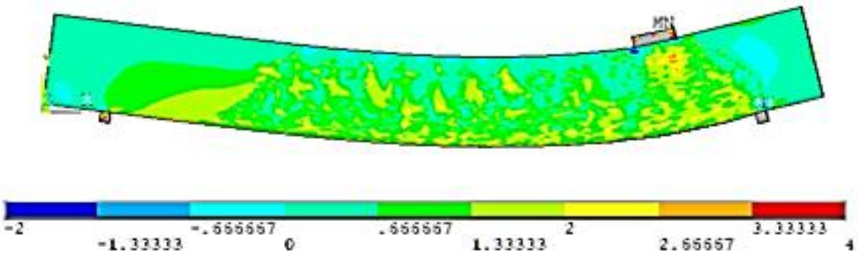
MN
-2
-1.33333
-.666667
0
.666667
1.33333
2
2.66667
3.33333
4

(B5)

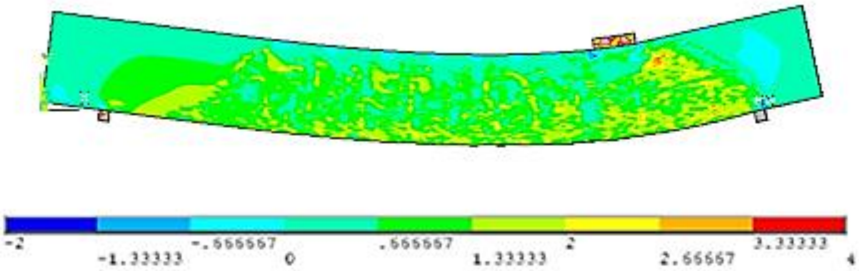

(B6)

Figure 4: Principal stress distribution at failure (MPa)

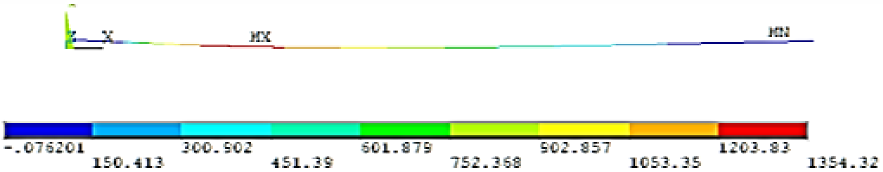
X
MX
MN
-.076201
150.413
300.902
451.39
601.879
752.368
902.857
1053.35
1203.83
1354.32

(B1)

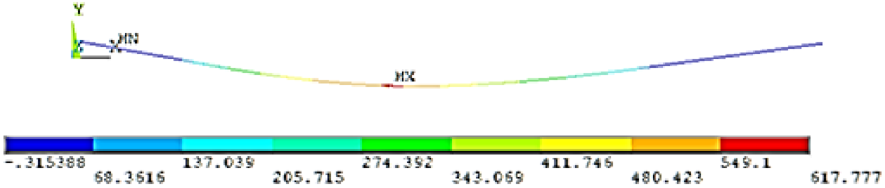
Y
X
MN
MX
-.315388
68.3616
137.039
205.715
274.392
343.069
411.746
480.423
549.1
617.777

(B2)

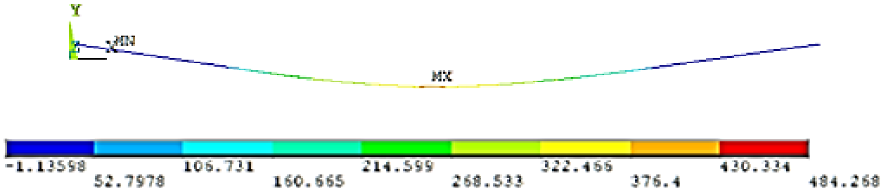
Y
X
MN
MX
-1.13598
52.7978
106.731
160.665
214.599
268.533
322.466
376.4
430.334
484.268

(B3)

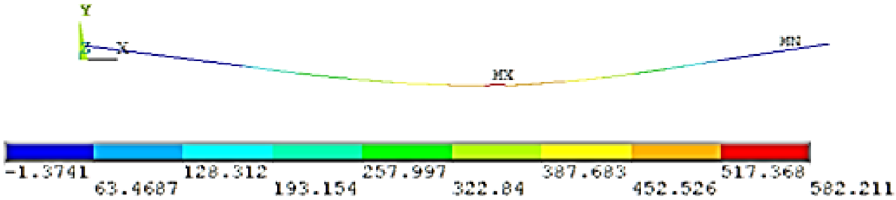
Y
X
MX
MN
-1.3741
63.4687
128.312
193.154
257.997
322.84
387.683
452.526
517.368
582.211

(B4)

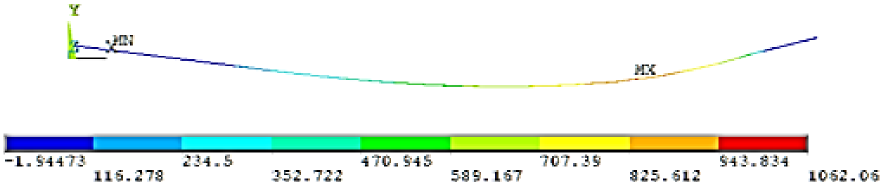
Y
X
MN
MX
-1.94473
116.278
234.5
352.722
470.945
589.167
707.39
825.612
943.834
1062.06

(B5)

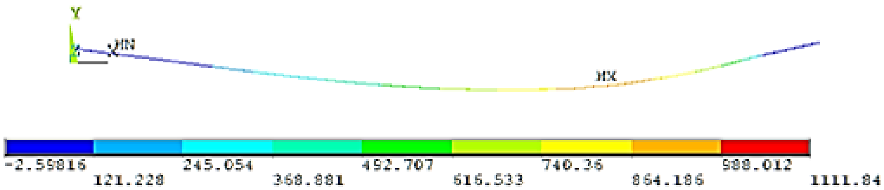

(B6)

Figure 5: Axial stress distribution in the CFRP bars at failure (MPa)